In Vivo Uptake of Radiolabeled Antibody to Proliferating Smooth Muscle Cells in a Swine Model of Coronary Stent Restenosis

Lynne L. Johnson, Lorraine M. Schofield, Stephen A. Verdesca, Barry L. Sharaf, Russell M. Jones, Renu Virmani, and Ban An Khaw

Division of Cardiology, Department of Medicine, Rhode Island Hospital, Providence, Rhode Island; Armed Forces Institute of Pathology, Washington, DC; and Northeastern University, Boston, Massachusetts

Z2D3 is a monoclonal chimeric antibody fragment that is directed against a protein expressed on the surface of proliferating smooth muscle cells. The purpose of this study was to investigate the uptake of ^{111}In-labeled Z2D3 F(ab')$_2$ in a swine model of coronary neointimal proliferation after overexpansion coronary stenting. **Methods:** Twenty-two domestic swine underwent overexpansion coronary stenting of 2 vessels. Fifteen swine survived 2–4 wk, at which time they received an injection of ^{111}In Z2D3 F(ab')$_2$ and underwent planar imaging. After the swine were killed, the hearts were excised and imaged on the detector. The cross-sectional area of each stented vessel was measured with digital morphometry. **Results:** Pathology could be correlated with imaging for 24 vessels. The cross-sectional area of stenosis comprising neointimal proliferation ranged from 8% to 95%, with a mean ± SD of 41% ± 21%. The maximal stenosis ranged from 13% to 95%, with a mean of 51% ± 20%. Seventeen of 24 vessels (71%) showed focal uptake on in vivo imaging, and 7 of 24 (29%) did not. Twenty of 24 (83%) showed uptake on ex vivo imaging. Of 11 stented vessels with maximal vessel stenosis less than 50%, 7 (64%) showed uptake both in vivo and ex vivo, and of 13 stented vessels with maximal vessel stenosis greater than 50%, 10 (77%) showed uptake both in vivo and ex vivo. **Conclusion:** Uptake of a radiolabeled antibody directed against a component of proliferating neointimal tissue can be visualized in the coronary arteries on in vivo imaging using a scintillation gamma camera.

Key Words: coronary stents; restenosis; swine; monoclonal antibodies

J Nucl Med 2000; 41:1535–1540

Despite improvements in the technique of balloon angioplasty and improvement in success rates, restenosis remains a major limitation, occurring in about 1 of 3 patients in the first 6 mo after the procedure. Stenting of coronary vessels has been increasingly used to overcome some of the limitations of balloon dilatation alone, but intracoronary stent placement is also associated with a restenosis rate of approximately 15%–20%. After intracoronary stenting, neointimal proliferation of smooth muscle cells is the major factor leading to coronary restenosis (*1*). Radiolabeling of antibody fragments provides markers that can target cells in vivo and identify disease processes. Z2D3 is a mouse and human chimeric antibody that binds an antigen expressed by proliferating smooth muscle cells in human atheroma. Narula et al. (*2*) investigated the uptake of various Z2D3 isotope preparations in rabbits and found localization in experimentally induced atheroma. The purpose of our study was to evaluate the uptake of ^{111}In-labeled Z2D3 F(ab')$_2$ in a swine model of coronary stenosis after oversized stent placement by correlating the results of in vivo imaging with the presence and extent of neointimal proliferation of the stented vessels on histopathology.

Received May 24, 1999; revision accepted Nov. 1, 1999.

For correspondence or reprints contact: Lynne L. Johnson, MD, Rhode Island Hospital Main Bldg., Rm. 208, 593 Eddy St., Providence, RI 02903.

MATERIALS AND METHODS

Antibody Preparation

F(ab')$_2$ fragments of the chimeric immunoglobulin G (IgG) antibody Z2D3 were prepared in the following way. Isolated, homogenized, postmortem human atheromatous plaques were used to develop murine monoclonal antibodies. The parent Z2D3 was then further engineered. First, a mouse and human chimeric IgG antibody was produced, and the whole antibody was broken by pepsin digestion into F(ab')$_2$ fragments. The immunoreactivity of this chimeric IgG fragment is similar to the parent IgM antibody. The F(ab')$_2$ fragments were then further modified to bind to the radiotracer, ^{111}In chloride. To decrease nonspecific cell binding and increase the specific activity of the radiolabeled antibody fragment, a negatively charged polymer (polylysine) was linked with multiple diethylenetriaminepentaacetic acid molecules and succinylated and conjugated to the chimeric Z2D3 F(ab')$_2$ fragments (*3*).

Stent Placement

This study was performed within the guidelines specified by the National Institutes of Health for the care and use of laboratory animals and with the approval of the Rhode Island Hospital Animal Care Committee. Twenty-two castrated male domestic swine (mean weight, 32.3 ± 8.6 kg) were studied. Each pig was given 325 mg acetylsalicylic acid and 120 mg verapamil 1 d before the

procedure to prevent coronary artery spasm. For the procedure, each pig was intubated and ventilated with a mixture of isoflurane, O_2, and nitrous oxide to maintain a level of anesthesia adequate to prevent the limb withdrawal reflex. Continuous echocardiographic monitoring was performed. Heparin (5000 U) was given as an intravenous bolus, and coronary angiography was performed through the right carotid artery with 8-French guiding catheters. The vessel diameter was estimated using the catheter diameter as a standard, and balloons and stents with a diameter approximately 20%–30% greater than the artery were chosen. Through a guiding catheter, a stent mounted on a balloon catheter was advanced into the left anterior descending (LAD) artery, left circumflex artery (LCF), or right coronary artery (RCA). The balloon was inflated 2 times at 6–10 atm for 20 s and then withdrawn, leaving the stent in place. Two stents were placed in each of 2 separate arteries in each animal. Coronary angiography was repeated to check stent placement and vessel patency. All catheters were removed, cutdowns repaired, and pigs allowed to recover and maintained on a regular diet for 14–28 d.

Injection and Imaging

All surviving animals underwent antibody injection and imaging at 14–28 d after stent placement. In 1 experiment, the animal was not injected with antibody and did not undergo imaging but received an injection of 50 mg/kg BrDU 1 h before being killed. Tissue was processed for immune staining.

Blood pool clearance of ^{111}In-Z2D3 F(ab′)$_2$ was calculated in the first experiment, and the half-time for the major component was 114 min. These data are consistent with the clearance data of ^{111}In antibody fragments in other species. Imaging was delayed 12–18 h after injection to allow blood-pool activity to fall below 20% of peak activity. Twenty-four hours before imaging, the dose of radiolabeled antibody was prepared. In the initial 10 experiments, the labeling was by direct mixing and incubation, but this method resulted in progressively poorer labeling efficiency (a decrease from 85% to 50%). Therefore, for the last 5 experiments, G-25 column chromatography (Sephadex; Sigma, St. Louis, MO) was used to separate bound antibody from free ^{111}In. To 1 aliquot of ^{111}InCl (approximately 2 mCi), an equal volume of 1 mol/L sodium citrate (pH 5.5) (100 μL) was added, followed by 1 aliquot of charge-modified Z2D3 F(ab′)$_2$ (139 μg). The reaction mixture was incubated for 30–45 min, and the ^{111}In-bound antibody was separated from free ^{111}In using G-25 column chromatography. The peak tube in the void volume was used as the dose. In 1 experiment, 100 μg nonspecific IgG was added to ^{111}In-citrate, and the dose was prepared using G-25 column chromatography. Serial elutions were collected, the first peak containing the Z2D3 bound with ^{111}In was used as the dose, and the peak with free ^{111}In was discarded. The animals were anesthetized with intramuscular Telazol (Elkins-Sinn, Cherry Hill, NJ) and xylazine, and the radiolabeled antibody was injected into an ear vein.

On the next morning, the animals were again anesthetized with Telazol and xylazine, an ear vein was cannulated, and the animals were intubated and maintained on thiopental sodium during imaging. Fluoroscopy was performed to observe and record stent placement. Imaging was then performed using a small-field-of-view gamma camera (Technicare Omega 420/CardioMac; NC Systems, Boulder, CO) with a medium-energy collimator and the 173- and 247-keV photopeaks of ^{111}In. Ten-minute planar images were obtained in projections selected to best separate the 2 stents.

The animals were killed with an overdose of thiopental sodium and KCl, and the hearts were rapidly excised. The hearts were imaged on the gamma camera detector for 30–40 min in projections approaching the projections used in vivo.

Scan Interpretation

The scans were interpreted in the following way. Focal uptake corresponding to regions of stented vessels was read on a scale of 1+ to 3+. Uptake that was greater than background activity but required contrast enhancement, and that could not be clearly seen in all views but was confirmed by ex vivo scans, was scored 1+. Uptake that was clearly apparent on all views with contrast enhancement was scored as 2+. Uptake that could be seen on unprocessed planar scans was scored as 3+. Images were enhanced by subtracting the background activity and lowering the upper threshold.

Pathology

The hearts were removed and fixed in formalin. The stented coronary arteries were carefully dissected, and the stent and surrounding artery were removed as a whole, processed in a graded series of alcohol, embedded in methyl methacrylate, and sawed into 1-mm segments from the proximal, middle, and distal portions of the stented artery. The 1-mm segments were cut with a carbide knife into 4-μm segments. (*4*) The sections were stained with hematoxylin-eosin and Movat pentachrome. The mean cross-sectional area of each stented section was measured using digital morphometry. The mean area was calculated as the average of 3 sections through the stent (proximal, mid, and distal). The percentage stenosis for each stent section was calculated as the area within the internal elastic lamina (IEL) minus the area of the residual lumen divided by the IEL area × 100. The neointimal area was calculated as the IEL area minus the area of the residual lumen. In addition, the greatest percentage of vessel stenosis was calculated from the smallest residual lumen area and the IEL area.

In the 1 experiment without injection and imaging, the animal was killed 14 d after stent placement. The animal received a 50 mg/kg 5-bromo-2-deoxyuridine (BrDU) (*5–7*) injection both at 24 h and immediately before being killed. In addition to the sectioning through the region of the stent for estimating neointimal thickening, the stent was removed from adjacent sections, and the tissue was dehydrated in alcohol and embedded in paraffin. Sections were stained with monoclonal antibodies to smooth-cell–specific actin.

RESULTS

Stent Placement

Of the 23 animals undergoing stent placement, 2 died during stent deployment because of acute vessel occlusion and 5 were found dead in their cages within 4 h after stent deployment. Fifteen animals that survived successful stent placement received an injection of radiolabeled antibody, were imaged, and were killed. Thirty oversized stents were placed in these 15 animals (12 LAD artery, 13 RCA, 5 LCF). The first 5 animals received homemade stents fashioned of wire wrapped around the balloon catheter. The remaining 10 animals received commercial intracoronary stents. One stent embolized systemically at the time of placement, and the vessel appeared normal at pathologic examination. One vessel was totally occluded by an organized thrombus. One vessel was used for autoradiography, and pathologic examination was therefore not performed. Tissue samples

from 3 additional stented vessels were lost and were not pathologically analyzed. The remaining 24 vessels were used to compare imaging and pathology results.

Imaging Results

Fifteen animals received an ^{111}In-Z2D3 F(ab')$_2$ injection, and 1 received an ^{111}In-IgG injection. The interval between stent placement and imaging for the first 4 experiments was approximately 4 wk, averaging 28 d, and the interval for the remaining 11 experiments was approximately 2 wk, averaging 14.8 d. Focal uptake of tracer was seen on in vivo imaging in the distribution of 6 of 9 RCAs, 7 of 10 LAD arteries, and 4 of 5 LCFs (Table 1). Four vessels showed 3+ uptake, 10 showed 2+ uptake, and 4 showed 1+ uptake. Overlying rib uptake of transchelated indium degraded image quality in several experiments, and multiple projections were obtained to identify any focal uptake in the regions of the stented vessels. High background activity may have contributed to the rate of false-negative findings; however, no correlation was found between scan positivity and radiotracer labeling efficiency.

In the experiment in which nonspecific radiolabeled antibody was injected, bone uptake was minimal and no focal tracer uptake could be seen in the region of the heart on in vivo planar imaging. On ex vivo imaging, faint tracer uptake was seen in the territory of the mid LAD artery stent.

TABLE 1
Imaging Results

Experiment no.	Vessel	Findings: In vivo	Findings: Ex vivo	Mean % stenosis	Maximum % stenosis	Comments
1	LCF	3+	NA	NA	36	
	RCA	−	NA	NA	NA	No path
6	LCF	−	+	8	16	
	RCA	−	−	NA	NA	No path
7	LAD	−	−	NA	NA	No path
	LCF	2+	+	28	49	
8	RCA	2+	+	42	67	
	LAD	−	+	47	54	
9	RCA	3+	+	22	32	
	LAD	3+	+	NA	NA	Autorads
11	RCA	−	−	100	100	Thrombus
	LCF	2+	+	44	52	
17	LAD	−	−	65	75	
	RCA	−	−	67	82	
19	LAD	2+	+	60	70	
	RCA	2+	+	53	66	
21	LAD	+	+	57	65	
	RCA	+	+	50	58	
22	LAD	2+	+	95	95	Thrombus
	LCF	+	+	21	23	
23	RCA	−	−	36	40	Embolized
	LAD	+	+	65	66	
25	LAD	3+	+	11	13	
	RCA	−	−	Normal	Normal	Embolized
26	LAD	2+	+	32	45	
	RCA	2+	+	31	52	
28	LAD	−	+	28	33	
	RCA	2+	+	22	37	
30	LAD	2+	+	33	50	
	RCA	−	+	37	42	

+ = positive; NA = not applicable; − = negative; No path = pathologic examination not performed; Autorads = vessel used for autoradiography.

Correlation with Pathology

Pathology and imaging data are displayed in Table 1 and Figures 1 and 2. Of the 30 vessels stented, 26 were examined pathologically. One vessel was totally occluded by an organized thrombus, and no tracer uptake was seen on either in vivo or ex vivo imaging. One vessel with an embolized stent was normal. Excluding these 2 vessels, the mean cross-sectional area of vessel stenosis comprising neointimal proliferation ranged from 8% to 95%, with a mean value of 41% ± 21%, and the maximal vessel stenosis ranged from 13% to 95%, with a mean value of 51% ± 20%. Of the 24 stented vessels showing neointimal thickening, 17 (71%) showed focal tracer uptake on in vivo imaging and 7 (29%) did not. Twenty (83%) showed uptake on ex vivo imaging. Of the 11 stented vessels with maximal vessel stenosis less than 50%, 7 (64%) showed focal tracer uptake both in vivo and ex vivo, and the smallest maximal vessel stenosis that showed uptake was 13%. Six of 7 stented vessels with less than 50% maximal vessel stenosis and positive findings showed 2+ to 3+ uptake. Ten of 13 stented vessels (77%) with more than 50% maximal luminal percentage stenosis showed focal tracer uptake both in vivo and ex vivo, and 7 of 10 scans with positive findings showed 2+ to 3+ uptake. The 7 stented vessels that had negative scan findings in vivo had maximal vessel stenoses ranging from 16% to 82% and included 3 LAD artery stents, 3 RCA stents, and 1 LCF stent.

Maximal vessel stenosis for the stented vessel stained for smooth muscle cell actin and BrDU was 38%. Five percent of actin-positive cells in the neointima were BrDU-positive. (Fig. 3)

No correlation was seen between scan positivity and time from stent placement to imaging, but no numbers are small. Six of 7 vessels showing neointimal thickening without tracer uptake were in animals imaged 14 d after stent placement, whereas 3 vessels showing 2+ uptake were in animals imaged late (>28 d).

DISCUSSION

Uptake of a radiolabeled antibody directed against a smooth muscle cell component of neointimal proliferating tissue in coronary arteries was visualized on in vivo imaging using a scintillation gamma camera in experimental animals. Stenting of coronary vessels has been increasingly used to overcome some of the limitations of balloon angioplasty, but intracoronary stent placement is also associated with a restenosis rate of approximately 15%–20% (*8,9*). Patients at highest risk for development of restenosis after stent placement include those with diabetes, a proximal LAD artery location, bifurcation lesions, total occlusions, and vein grafts

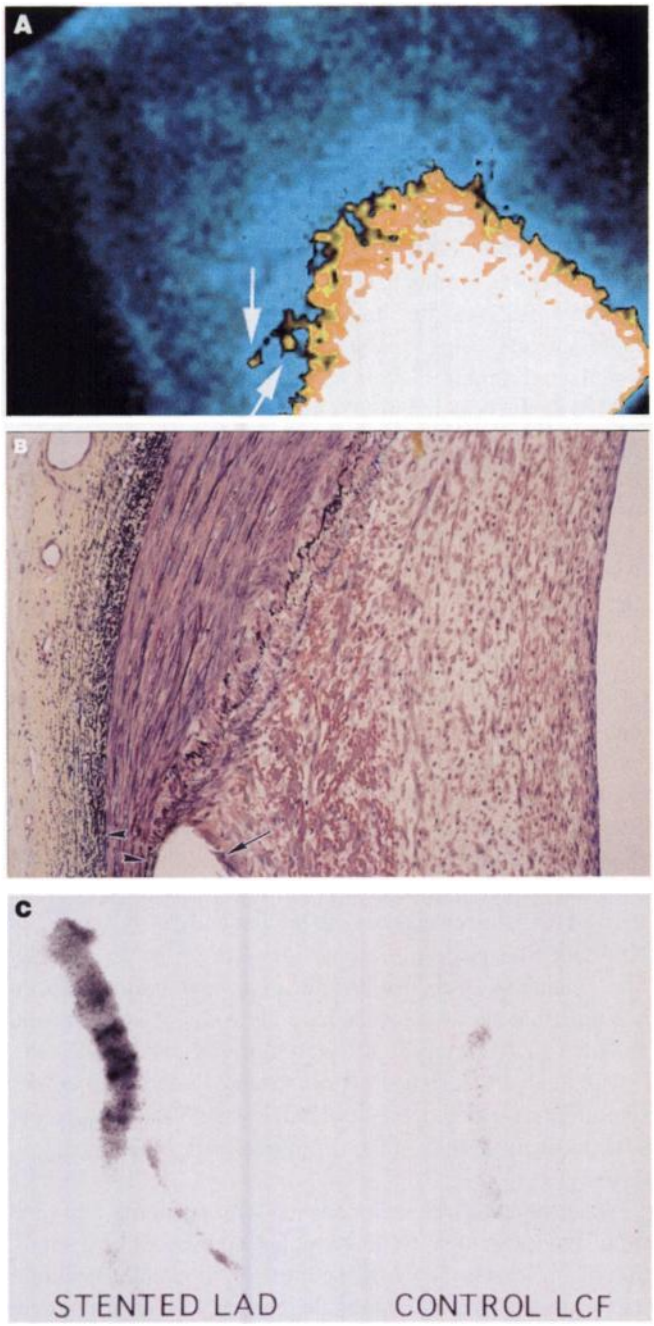

FIGURE 1. Scans, cryostat sections, and autoradiographs 14 d after stent deployment in experiment 9. (A) Left anterior oblique angled planar scan shows tracer uptake (arrows) in proximal portions of LAD artery and RCA. (B) Photomicrograph shows stent artifact (arrow), normal media to left, with internal and external laminas (arrowheads) beneath thick neointima rich in smooth muscle (Movat pentachrome, ×40). (C) Autoradiographs of LAD artery from same experiment show uptake in region of stented vessel on left and no uptake in control vessel (LCF) on right.

(*10*). Whereas vascular remodeling is the major factor leading to coronary restenosis after balloon angioplasty, neointimal proliferation of medial smooth muscle cells is the major factor after intracoronary stenting (*11–13*).

Schwartz et al. (*14,15*) developed a swine model in which extensive neointimal proliferation occurred after fracture of the coronary artery IEL because of an overexpanded coil. They developed the technique of delivering metal wire coils wrapped around high-pressure balloons into the coronary arteries of domestic swine. The diameters of the inflated balloons were selected to be greater than the vessels in which they were deployed. The intent of this procedure was

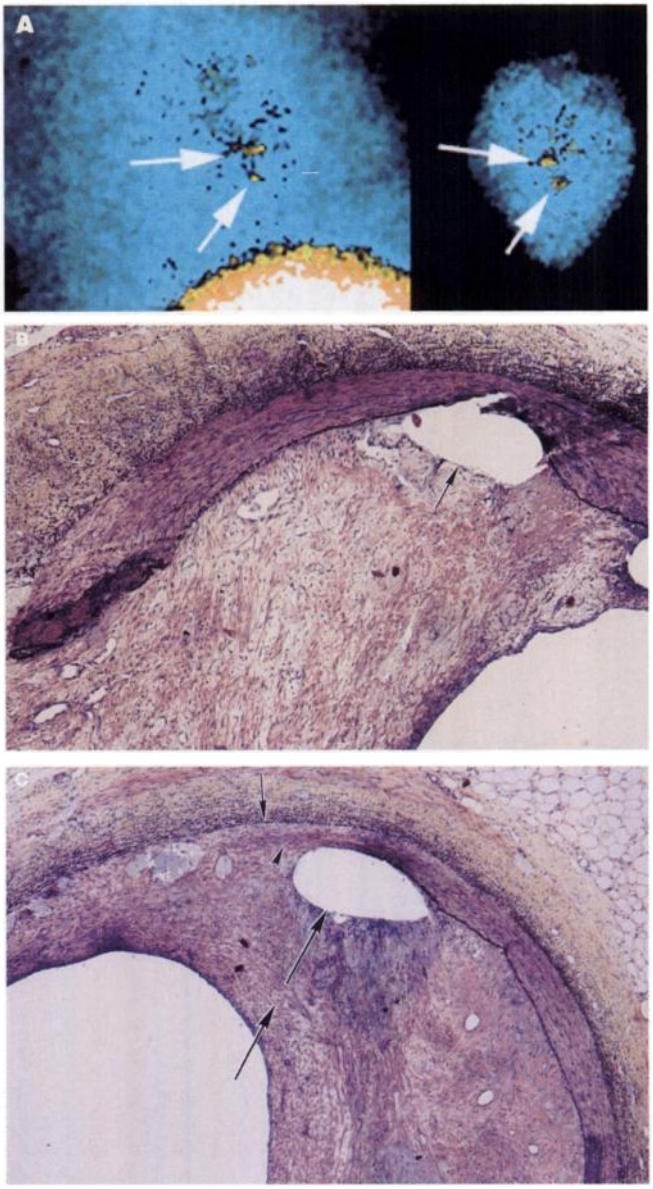

FIGURE 2. Scans and cryostat sections of LAD artery and RCA 14 d after stent deployment in experiment 26. (A) On left, oblique angled planar scan shows tracer uptake (arrows) in proximal portions of LAD artery and mid RCA; on right, ex vivo imaged heart shows corresponding regions of focal uptake (arrows). Base of heart is at top of image. (B) View of thick, organizing thrombus layer covering stent (arrow) in LAD artery shows total cleavage of medial layer and thickened adventitia (Movat pentachrome, ×20). (C) Thick, organizing thrombus is seen covering stent (large arrow) in RCA. Media shows IEL disruption (arrowhead) beneath stent void and intact external elastic lamina (small arrow) (Movat pentachrome, ×10).

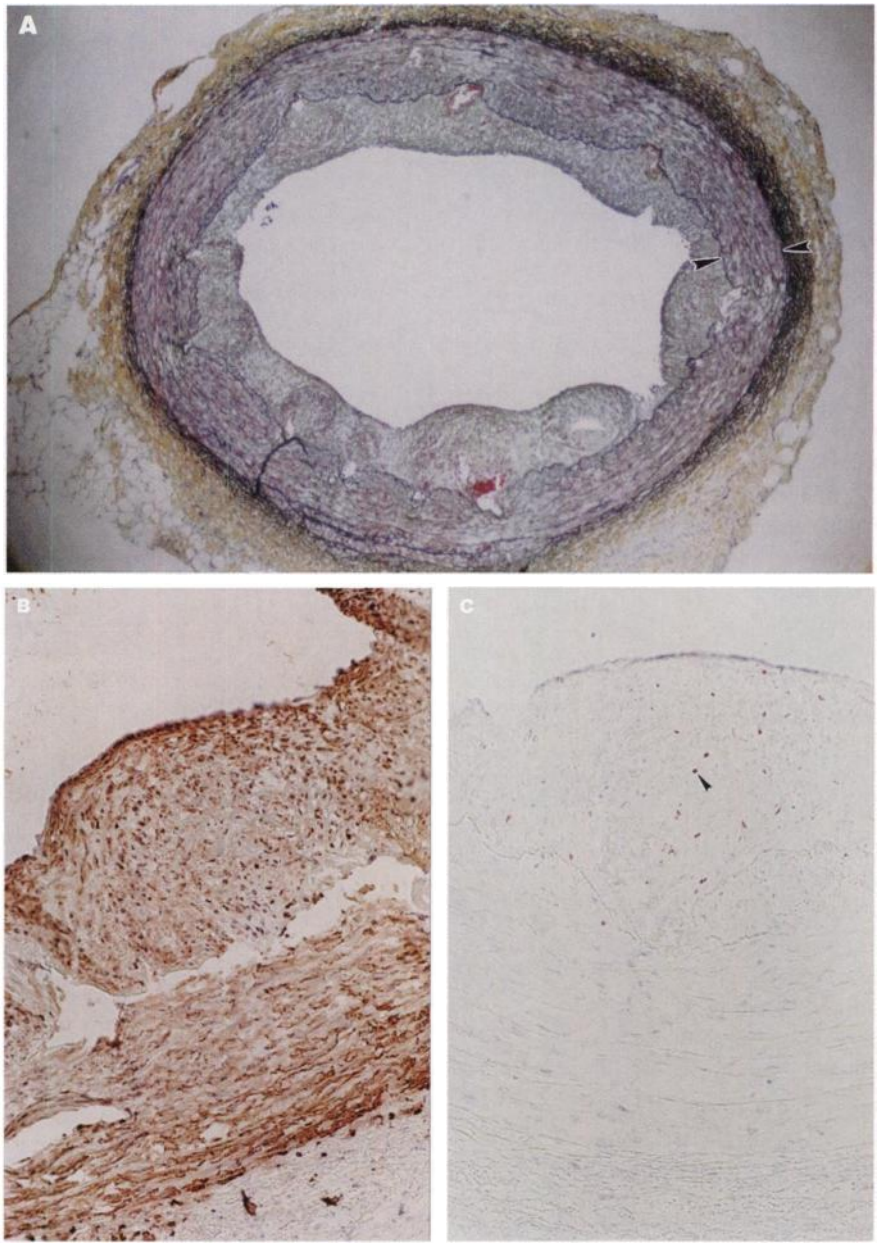

FIGURE 3. Serial cryostat sections of LAD artery 14 d after stent deployment. Sections were prepared after removal of stent wires. (A) Low-power cross-section stained using Movat pentachrome methods (×4) shows intimal lesion. IEL and external elastic lamina are identified with arrowheads. (B) Identification of smooth muscle cells with monoclonal antibody HHF-35 shows intense immunoreactivity (red reaction product) in media and neointima (×40). (C) Immunostaining with monoclonal antibody directed against bromodeoxyuridine (BrDU) in area similar to that in (B) (×40). BrDU labeling represents active cell proliferation and colocalization of most positive nuclei (arrowhead) with actin-positive smooth muscle cells in developing neointima. (B) and (C) were counterstained with Gill's hematoxylin, yielding blue nuclei.

to rupture the IEL and stimulate smooth muscle cell proliferation. Those investigators and others subsequently applied this model to the evaluation of therapeutic interventions that might affect restenosis after angioplasty.

The pathologic hallmark of restenosis after coronary stent placement in man and after stent overexpansion vascular injury in swine is neointimal proliferation comprised predominantly of smooth muscle cells and matrix. Narula et al. (*2*) showed uptake of radiolabeled fragments of the mouse and human chimeric monoclonal antibody Z2D3 $F(ab')_2$ in experimentally induced atheroma in rabbit aorta. Comparative immunohistologic studies using proliferating cell nuclear antigen (PCNA)—a nuclear protein cofactor for DNA polymerase delta that identifies cells undergoing replication—and an antibody specific for smooth muscle α actin showed that Z2D3 $F(ab')_2$ identified proliferating smooth muscle cells and not macrophages in rabbit aorta (*2*). This study also showed that in the rabbit model, the proliferation of smooth muscle cells peaked at 7 d. The antigen homologous for Z2D3 $F(ab')_2$ antibody has not been completely characterized, but the epitope is thought to be a complex of 2 or more chemically dissimilar, low-molecular-weight molecules produced by proliferating smooth muscle cells.

The extent of neointimal thickness does not reflect the rate of smooth muscle cell proliferation. Using PCNA and immunolocalization of PCNA, Carter et al. (*4*) characterized the time course and extent of cell proliferation in the intima and media of the vessel wall in a similar swine model. These investigators found that maximal smooth muscle cell proliferation occurs at 7 d, with a decline to low levels at 28 d. Because Z2D3 $F(ab')_2$ binds to actively proliferating smooth muscle cells, the false-negative findings in this study may be

caused by low rates of smooth muscle cell proliferation at the time of antibody injection and imaging. Likewise, the more strongly positive findings seen in vessels with relatively smaller degrees of neointimal proliferation may be caused by higher rates of smooth muscle cell proliferation in these vessels. This small sample size lacked correlation between the interval from stent placement to tracer injection and scan positivity. Six of 7 vessels showing neointimal thickening without tracer uptake were in animals imaged 14 d after stent placement, and 3 vessels showing 2+ uptake were in animals imaged late (28 d). In the 1 experiment in which BrDU, a nucleotide analog that is incorporated into actively replicating DNA, was injected, 5% positive-stained cells for DNA synthesis were seen in sections also staining for actin at 14 d after stent placement. Few data are available in the literature using animal models of restenosis and BrDU. In a rabbit model of deendothelialized arteries, the percentage of neointimal BrDU-labeled smooth muscle cells was 33% ± 23%, with a range of 8%–66% at 8 d (*16*). Further studies are necessary to investigate the relationship between radiotracer uptake and rates of smooth muscle cell proliferation in this model.

Potential difficulties exist in using animal models when studying the histopathology of human disease. Stents are deployed into human coronary arteries that have advanced degrees of atherosclerotic plaque formation, whereas in the porcine model of overexpansion restenosis the vessels are not diseased and the stimulus to neointimal proliferation is the vascular injury caused by the stent placement.

^{111}In uptake by bones (ribs) interfered with good visualization of the proximal coronary vessels and contributed to difficulties in localizing uptake in vivo in some animals. The cause for this nonspecific (bone) uptake of indium is probably transchelation of indium to transferrin. This limitation may be overcome using either a different radioisotope or a different chelator. SPECT, which was not performed, would have improved contrast resolution and allowed better visualization of tracer obscured by overlying bone uptake of ^{111}In.

CONCLUSION

These findings are preliminary, and further work is necessary to improve antibody specificity and imaging quality and to investigate the relationship between radiotracer uptake and rates of smooth muscle cell proliferation. This study shows that atherosclerotic lesions of the coronary arteries can be visualized in vivo in a large-animal model. The low sensitivity and, in many cases, poor image quality are caused by biologic factors (varying rates of smooth muscle cell proliferation) and imaging techniques. However, the results show evidence of the concept and suggest that by applying current state-of-the-art technology, visualization of atherosclerotic processes in the coronary arteries may be feasible. A noninvasive method to detect restenosis may be useful in evaluating the effects of new prevention methods and in identifying patients who need repeated intervention before symptoms or an ischemic event has occurred (*17–19*).

ACKNOWLEDGMENT

This study was supported by a grant-in-aid from the Rhode Island affiliate of the American Heart Association.

REFERENCES

1. Karas SP, Gravanis MB, Santoian EC, Robinson KA, Anderberg KA, King SP. Coronary intimal proliferation after balloon injury and stenting in swine: an animal model of restenosis. *J Am Coll Cardiol.* 1992;20:467–474.
2. Narula J, Petrov A, Bianchi C, et al. Noninvasive localization of experimental atherosclerotic lesions with mouse/human chimeric Z2D3 F(ab')$_2$ specific for the proliferating smooth muscle cells of human atheroma. *Circulation.* 1995;92:474–484.
3. Torchilin VP, Klibanov ND, Nossiff MA, et al. Monoclonal antibody modification with chelate-linked high molecular weight polymers: major increases in polyvalent cation binding without loss of antigen binding. *Hybridoma.* 1987;6:229–240.
4. Carter AJ, Laird JR, Farb A, Kufs W, Wortham DC, Virmani R. Morphologic characteristics of lesion formation and time course of smooth muscle cell proliferation in a porcine proliferative restenosis model. *J Am Coll Cardiol.* 1994;24:1398–400.
5. Dolbeare F. Bromodeoxyuridine: a diagnostic tool in biology and medicine. Part I. Historical perspectives, histochemical methods and cell kinetics. *Histochem J.* 1995;27:339–369.
6. Dolbeare F. Bromodeoxyuridine: a diagnostic tool in biology and medicine. Part II. Oncology, chemotherapy and carcinogenesis. *Histochem J.* 1995;27:923–964.
7. Dolbeare F. Bromodeoxyuridine: a diagnostic tool in biology and medicine. Part III. Proliferation in normal, injured and diseased tissue, growth factors, differentiation, DNA replication sites and in sites in situ hybridization. *Histochem J.* 1995;28:531–575.
8. Serruys PW, DeJaegere P, Kiemenej F, et al, for the Benestent Study Group. A comparison of balloon-expandable stent implantation with balloon angioplasty in patients with coronary artery disease. *N Engl J Med.* 1994;331:489–495.
9. Fischman DL, Leon MB, Baim DS, et al, for the Stent Restenosis Study Investigators. A randomized comparison of coronary-stent placement and balloon angioplasty in the treatment of coronary artery disease. *N Engl J Med.* 1994;331:496–501.
10. Kastrati A, Schomig A, Elezi S, et al. Predictive factors of restenosis after coronary stent placement. *J Am Coll Cardiol.* 1997;30:1428–1436.
11. Austin GE, Ratliff NB, Hollman J, Tabei S, Phillips DF. Intimal proliferation of smooth muscle cells as an explanation for recurrent coronary artery stenosis after percutaneous transluminal coronary angioplasty. *J Am Coll Cardiol.* 1985;6:369–375.
12. Kirmura T, Kaburagi S, Tamura T, et al. Remodeling of human coronary arteries undergoing coronary angioplasty or atherectomy. *Circulation.* 1997;96:475–483.
13. Isner JM. Vascular remodeling: honey, I think I shrunk the artery. *Circulation.* 1994;89:2937–2941.
14. Schwartz RS, Murphy JG, Edwards WD, Camrud AR, Vlietstra RE, Holmes DR. Restenosis after balloon angioplasty: a practical proliferative model in porcine coronary arteries. *Circulation.* 1990;82:2190–2290.
15. Schwartz RS, Edwards WD, Antoniades LC, Bailey KR, Holmes DR. Coronary restenosis: prospects for solution and new perspectives from a porcine model. *Mayo Clin Proc.* 1993;68:54–62.
16. Verin V, Popowski Y, Urban P, et al. Intra-arterial beta irradiation prevents neointimal hyperplasia in a hypercholesterolemic rabbit restenosis model. *Circulation.* 1995;92:2284–2290.
17. Teirstein PS, Massullo V, Jani S, et al. Catheter-based radiotherapy to inhibit restenosis after coronary stenting. *N Engl J Med.* 1997;336:1697–1703.
18. Schwartz RS, Koval TM, Edwards WD, et al. Effect of external beam irradiation on neointimal hyperplasia after experimental coronary artery injury. *J Am Coll Cardiol.* 1992;19:1106–1113.
19. Wiedermann JG, Marboe C, Amols H, Schwartz A, Weinberger J. Intracoronary irradiation markedly reduces restenosis after balloon angioplasty in a porcine model. *J Am Coll Cardiol.* 1994;23:1491–1498.